Research Article
https://doi.org/10.1631/jzus.B2300652

SLC2A3 promotes colorectal cancer metastasis by triggering the YAP-1/PDGFB axis

Jinlong TANG[1*], Minglang MAI[2*], Fengyan HAN[3], Chaoyi CHEN[4,5], Shuli XIA[6], Xueping XIANG[1], Qi YANG[1], Kefeng DING[4,5]✉

[1]*Department of Pathology, the Second Affiliated Hospital of Zhejiang University School of Medicine, Hangzhou 310009, China*
[2]*Key Laboratory of Disease Proteomics of Zhejiang Province, Hangzhou 310058, China*
[3]*School of Basic Medical Sciences, Guangzhou Medical University, Guangzhou 511436, China*
[4]*Department of Colorectal Surgery and Oncology, Key Laboratory of Cancer Prevention and Intervention, Ministry of Education, The Second Affiliated Hospital, Zhejiang University School of Medicine, Hangzhou 310009, China*
[5]*Cancer Center of Zhejiang University, Hangzhou 310009, China*
[6]*Zhejiang Provincial Hospital of Traditional Chinese Medicine, Hangzhou 310003, China*

Abstract: Distant metastasis and dissemination are the leading contributors to colorectal cancer (CRC) death. The underlying biomechanisms by which the SLC2A3 promotes CRC aggression still need to be comprehensively clarified. Data on SLC2A3 expression in normal and tumor tissues from the Gene Expression Omnibus (GEO) and the Cancer Genome Atlas (TCGA) databases were analyzed. Prognostic values were assessed using a Kaplan–Meier analysis. The construction of overexpressed and knockout cell lines of SLC2A3 was performed using the CRISPR-Cas9 system. Biological functions, including migration and invasion, were detected using a transwell assay. SLC2A3 subcellular location was determined using immunofluorescence staining. Signaling pathway analysis was accomplished by RNA sequencing and GO pathway enrichment. SLC2A3 downstream effectors were validated via qRT-PCR and Western blotting after gene interference and overexpression. Furthermore, SLC2A3 and related proteins in CRC tissues were detected by immunohistochemistry. The in vivo mouse xenograft model was performed to assess distant lung metastasis. Finally, the clinicopathological features, prognostic values, and correlations between SLC2A3 and associated molecules were analyzed using the Chi-square test, Spearman's rho model, and Kaplan–Meier analysis. The results showed that SLC2A3 was markedly up-regulated in CRC samples and linked to adverse outcomes. We also demonstrated that SLC2A3 promotes CRC migration and invasion in vitro, which is involved in pathways associated with cancer and cytokine–cytokine receptor interaction. We confirmed that SLC2A3 accelerates CRC migration and invasion by activating the YAP-1/PDGFB axis. Furthermore, we validated that PDGFB facilitates CRC migration and invasion. Moreover, the in vivo mouse xenograft studies confirmed that SLC2A3 promoted CRC cells distant lung metastasis by activating the YAP-1/PDGFB axis. High SLC2A3, YAP-1, and PDGFB expressions in the CRC tissues were significantly correlated with lymph node metastasis, nervous invasion, lymphovascular invasion, distant metastasis, and pTNM stage, respectively. There was a correlation with the expression of SLC2A3, YAP-1, and PDGFB in CRC tissues, and high expression of them was a hazard factor for CRC. Taken together, SLC2A3 serves as an oncogene to promote CRC aggression and is associated with adverse prognosis through positively simulating the YAP-1/PDGFB axis. It may be used as a potential biomarker of CRC prognosis and a prospective target for CRC treatment.

Key words: SLC2A3; Colorectal cancer; YAP-1; PDGFB; Prognosis

✉ Kefeng DING, dingkefeng@zju.edu.cn
* The two authors contributed equally to this work.
Kefeng DING, https://orcid.org/0000-0002-2380-3717
Jinlong TANG, https://orcid.org/0000-0002-9564-900X

Received Sept. 13, 2023; Revision accepted Mar. 6, 2024;
Crosschecked xxx. xx, 20xx; Published online xxx. xx, 20xx

© Zhejiang University Press 2024

Uncorrected

1 Introduction

Colorectal cancer (CRC) is one of the most common malignant tumors, ranking third in incidence and mortality (Siegel et al. 2022). Distant metastasis and dissemination were the leading contributors to CRC death, with approximately 25% of advanced CRC metastasizing to the liver and 5–18% to the lung, respectively (Eefsen et al. 2012; Parnaby et al. 2012); this was linked to cancer recurrence and a high burden of cancer-associated disability-adjusted life years (Global Burden of Disease Cancer et al. 2022). Hence, uncovering the underlying biomechanisms leading to CRC distant metastasis and dissemination may be of particular importance to CRC interventions and treatments, ultimately reducing mortality and improving the quality of life of patients.

SLC2A3 is a gene located on human chromosome 12p3.3 that encodes glucose transporter 3 (GLUT3) (Kayano et al. 1988), a member of the glucose transporter family composed of the 12-transmembrane domain containing α-helical domains with cytoplasmic amino (N)-termini and carboxy (C)-termini and displaying a higher affinity for glucose and a greater capacity to transport glucose from extracellular fluid across the plasma membrane into cytoplasm compared to other GLUTs (Simpson et al. 2008). During gestation, SLC2A3 expression was generally lower in the placenta due to high DNA promoter methylation (Novakovic et al. 2013). After birth, SLC2A3 has frequently been detected in normal human tissues, including brain tissue, testes, and placenta (Younes et al. 1997), and is widely involved in the pathophysiological process of various non-neoplastic diseases, such as Alzheimer's disease, schizophrenia, diabetes mellitus, ischemia, neurite outgrowth, etc. (An et al. 2018; Kang et al. 2018; Segarra-Mondejar et al. 2018; Fidler et al. 2019; Sullivan et al. 2019). Additionally, under pathological circumstances, SLC2A3 expression was aberrantly increased. It may contribute to proliferation, migration, invasion, distant metastasis, and poor prognosis in various malignant tumors, including testicular, ovarian, oral, esophageal, gastric, colorectal, thyroid, and lung cancers, as well as glioblastoma (Ayala et al. 2010; Jozwiak et al. 2012; Cosset et al. 2017; Martinez-Romero et al. 2018; Kim et al. 2019; Wu et al. 2020; Gao et al. 2021; Pan and Zang 2022). Many previous studies have therefore suggested that SLC2A3 plays a vital role in cancer initiation and malignant progression.

In CRC, previous studies showed that SLC2A3 expression was higher in tumor tissues than in adjacent normal colorectal tissues, which may be associated with tumor T stage, lymph node metastasis, TNM stage, and lymphatic invasion, thus contributing to the poor prognosis (Martinez-Romero et al. 2018; Kim et al. 2019; Wu et al. 2020; Gao et al. 2021). Moreover, increasing studies confirmed that the Yes-associated protein (YAP)-related Hippo pathway plays various roles in tumor initiation, growth, distant metastasis, prognosis, and drug resistance in various cancers (Liu et al. 2013; Akervall et al. 2014; Wang et al. 2014; Dubois et al. 2019; Yoo et al. 2019). YAP-1 may serve as an oncogene in CRC to enhance malignancy by interacting with multiple cofactors, including microRNA, long non-coding RNA, and transcription factors, which avoid YAP-1 degradation in the cytoplasm and facilitate YAP-1 to transfer into and exert its function in the nucleus (Sun et al. 2019; Yao et al. 2022). A recent study demonstrated that YAP may activate the SLC2A3/AMP-activated protein kinase (AMPK) signaling pathway to promote CRC aggression (Jiang et al. 2021). Another investigation also indicated that SLC2A3 could act as an oncogene to accelerate cancer cell invasion and lung metastasis by activating the YAP-related pathway (Kuo et al. 2019). However, the biomechanisms by which the SLC2A3-simulated YAP-related pathway promotes CRC aggression still need to be comprehensively clarified.

Platelet-derived growth factor B (PDGFB), a member of the platelet-derived growth factor family, is a polypeptide chain protein that can form a homodimer PDGFBB to directly bind with platelet-derived growth factor receptor ββ (PDGFR-ββ). PDGFBB generally plays a protective role in tissue injury and repair but, most importantly, angiogenesis, by recruiting pericytes and enhancing their motility via activating the SDF-1α/CXCR4 signaling pathway (Greenhalgh et al. 1990; Stavri et al. 1995; Song et al. 2009). Aberrantly high PDGFBB secretion could facilitate tumor cell proliferation, migration, bone, and lung metastasis by involving various signaling pathways, such as epithelial–mesenchymal transition (EMT) and the YAP-related Hippo pathway, which contribute to adverse prognosis in breast cancer, lung cancer, and pancreatic cancer (Yi et al. 2002; Neri et al. 2017; Hsu et al. 2019; Li et al. 2021). Moreover, recent data have suggested that PDGFBB is associated with the unfavorable prognosis of CRC by recruiting pericytes and enhancing angiogenesis, which makes it a potential biomarker for CRC diagnosis (McCarty et al. 2007; Nakamura et al. 2008; Ionescu et al. 2011). Nonetheless, whether SLC2A3 is associated with PDGFB regulation remains unclear, and the underlying molecular mechanisms should be further deciphered.

Uncorrected

Although SLC2A3 mainly acts as an oncogene in various cancers, including CRC, whether the underlying molecular biomechanisms by which SLC2A3 regulates colorectal cancer invasion and metastasis and the role of SLC2A3 involve PDGFB regulation remains unclear. In this study, we found that SLC2A3 played a causative role in CRC migration and invasion by over-activating the YAP-1/ PDGFB axis, which may contribute to CRC poor prognosis.

2 Materials and methods

2.1 Public database selection

The GSE68468, GSE44861, GSE44076, and GSE21510 gene expression databases of CRC were obtained from the Gene Expression Omnibus (GEO) (http://www.ncbi.nlm.nih.gov/geo; accessed on July 11, 2022) and the Cancer Genome Atlas (TCGA) databases (https://tcga-data.nci.nih.gov/tcga/; accessed on July 11, 2022). Survival data on CRC were obtained from TCGA datasets, the GSE17536 database (http://www.ncbi.nlm.nih.gov/geo; accessed on July 11, 2022), and the GSE38832 database (http://www.ncbi.nlm.nih.gov/geo; accessed on July 11, 2022). Statistically significant differences between the two groups were analyzed with GraphPad Prism 8.0 (GraphPad, Software, San Diego, CA, US).

2.2 Cell culture

The human CRC cell lines HCT116 and RKO were purchased from the American Type Culture Collection (ATCC) and were cultured in RPMI 1640 (Gibco, Shanghai, China). All media were supplemented with 10% fetal bovine serum (FBS; Gibco, Shanghai, China) and penicillin/streptomycin. Cell lines were incubated in a 5% CO_2 atmosphere at 37°C. Cells were treated with different concentrations of PDGFB reagent (Sino biological, Cat# 10572-H07Y) (50 ng/ml, 500 ng/ml, 5 μg/ml, and 50 μg/ml) for 24 hours.

2.3 Transfection of oligonucleotides and construction of vectors

Small interfering RNA (siRNA) oligonucleotides were purchased from SignaGen (Shanghai, China). Sequences of siRNAs were as follows: SLC2A3-homo-357 sene: GCUCUUUCCAAUUUGGCUATT; SLC2A3-homo-357 antisene: UAGCCAAAUUGGAAAGAGCTT. SLC2A3-homo-578 sene: GUAGCUAAGUCGGUUGAAATT; SLC2A3-homo-578 antisene: UUUCAACCGACUUAGCUACTT. SiRNAs were transfected with GenMute siRNA Transfection Reagent (SignaGen, Cat# SL100568). The plasmid vectors of pcDNA3.1+ empty vector (EV) and pcDNA3.1+-flag-SLC2A3 were transfected with LipoD293 (SignaGen, Cat# SL100668) according to the manufacturer's instructions. After 48 hours, cell mediums were refreshed, and cells were cultured for subsequent experiments.

2.4 SLC2A3 knockout (KO) cell lines

SLC2A3 KO cell lines in HCT116 were generated with the CRISPR-Cas9 system, and pLentiCRISPR v2 vector encoding a single-guide RNA (sgRNA) was transfected into the HCT116 cell line to downregulate SLC2A3 expression. Forty-eight hours later, puromycin (4 μg/mL) was fortified for 4 days consecutively in the transfected HCT116 cell line for clone selection. The selective puromycin-resistant single cell lines were separated, cultured, and reproduced over 6 days in a 96-well plate. Cloned cells without CRISPR-Cas9 edition were isolated as mock cells. KO effects were assessed by qRT-PCR and Western blot assays. sgRNA sequences were as follows: SLC2A3 sgRNA1: CACCGGACTCTTCGTCAACCGCTT; SLC2A3 sgRNA2: CACCGGCCTTTTCGTTAACCGCTT.

2.5 Western blotting

Total cells at the end of the experiments were collected and lysed using a RIPA buffer kit (Beyotime Institute of Biotechnology). Cell lysates were concentrated, and 30 μg protein samples were added and isolated in the 10% SDS–polyacrylamide gels, after transfer to a nitrocellulose membrane. Then, they were blocked in the 5% defatted milk solution at 37°C for 1 hour and incubated overnight at 4°C with primary antibodies against SLC2A3 (Abcam, Cat# ab41525), YAP-1 (Cell Signaling Technology, Cat# 14074T), and PGDFB (Affinity，Cat# AF0240). All these antibodies were diluted as 1:2000, and GAPDH was used as an internal control primary antibody (1:5000, Affinity, Cat# T0004). Then, second antibodies (1:5000, Invitrogen, Cat# 926-68070) were

Unedited

added and incubated at 4℃ for 1 hour. Finally, visualization was performed with the Odyssey system.

2.6 Cell migration and invasion

Transwell assays using 24-well transwell chambers were performed to analyze CRC cell migration and invasion; 100 μL serum-free RPMI 1640 medium containing 1×10^5 cells for the transwell assay was added to the upper chambers per well. Additionally, 600 μL RPMI 1640 medium with 10% FBS was added to the lower chambers per well as a chemoattractant. After being incubated for 24–48 hours, the cells left on the upper surface of the filter were cleared up, while the cells that passed through and settled on the bottom surface of the filter were fixed in 4% paraformaldehyde at 37℃ for 20 minutes, followed by staining with a 0.1% crystal violet solution at 37℃ for 15 minutes. Next, migration or invasive pictures of cells were photographed under the microscope. Then, cells were digested with 33% acetic acid and transferred into the 96-well plate for quantifying the absorbance at 570 nm with a microplate reader.

2.7 Quantitative Real-Time PCR (qRT-PCR)

Total RNAs were extracted from cells with TRIzol® reagent (Pufei, cat# 3101-100). cDNA synthesis was performed with the HiScript II Q RT SuperMix for qPCR (+gDNA wiper) (Vazyme, Cat# R223-01) according to the manufacturer's protocol. ChamQ Universal SYBR qPCR Master Mix (Vazyme, Cat# Q711-02) was used to perform qPCR on the Applied 480II-384 platform (Roche) according to the manufacturer's instructions. Specific relative gene expression normalized to GAPDH was analyzed using the $2^{-\Delta\Delta Cq}$ method (Livak and Schmittgen 2001). All primer information was as follows: SLC2A3 forward: TATCTTGGTCTTTGTAGCCTTCTTT; SLC2A3 reverse: AATGAGGAAGCCGGTGAAGATA. YAP-1 forward: AGTTACCAACACTGGAGCAGG; YAP-1 reverse: TTCGAGGGACACTGTAGCTG. PDGFB forward: TTCGAGGGACACTGTAGCTG; PDGFB reverse: AAAGATTGGCTTCTTCCGCAC. GAPDH forward: CCCTTCATTGACCTCAACTACATG; GAPDH reverse: TGGGATTTCCATTGATGACAAGC.

2.8 Immunofluorescence staining

Cells with SLC2A3-KO in HCT116 and SLC2A3-overexpressed in RKO and corresponding control cells were seeded and cultured on a sterilized slide in 6-well plates, respectively. After being washed with PBS three times, cells were fixed in 4% paraformaldehyde solution for 30 minutes and permeabilized with 0.5% Triton X-100 for 10 minutes at room temperature. Then, slides were blocked with 5% BSA (Amersco, USA)/PBST solution for 1 hour and incubated with a primary antibody against SLC2A3 overnight at 4℃. Subsequently, a fluorochrome-labeled anti-rabbit secondary antibody (1:500, Alexa Fluor 546 Goat anti-Rabbit IgG (H+L)) was added and incubated for 1 hour at room temperature. Then, cells were stained with DAPI reagent (1:5000, Invitrogen, Cat# D21490). Finally, fluorescence photography and merged images were captured with an OLYMPUS IX83-FV3000-OSR.

2.9 RNA sequencing and Gene Ontology pathway enrichment analysis

For RNA sequencing, the total RNAs of SLC2A3-KO HCT116 cells and SLC2A3 mock HCT116 cells were isolated, sequenced, and analyzed by RiboBio (Guangzhou, China). All groups were processed independently and this was repeated three times. An Illumina HiSeq 3000 sequencer was utilized to sequence paired-end libraries. The analysis of gene differential expression was performed with Cuffdiff in the Cufflinks package. Gene differential expressions, defined as $q < 0.05$ and $|\log2(\text{fold change})| > 0.8$, could then be analyzed and verified by quantitative PCR. GO pathway enrichment was analyzed using the online DAVID tool (http://david.abcc.ncifcrf.gov). The results were visualized with the R package ggplot2 analysis in the R software.

2.10 Clinical data

A total of 135 patients were diagnosed with CRC after surgical operation performed by at least two proficient pathologists at the Second Affiliated Hospital, Zhejiang University School of Medicine, from January 2007–December 2008. None of the CRC patients in the study received neoadjuvant chemotherapy or radiotherapy before surgery. The postoperative pathological diagnosis and staging were classified according to the 2019 WHO tumor classification and the American Joint Committee on Cancer (AJCC) TNM Staging Classification for Carcinoma of CRC, 8th edition. Patient and follow-up data were obtained from hospital records or

Unedited

telephone interviews. All patients provided informed consent under institutional review board-approved protocols, and the research was approved by the Human Research Ethics Committee of the Second Affiliated Hospital of Zhejiang University School of Medicine.

2.11 Construction of a xenograft mouse model

Ten four-week-old BALB/c nu/nu male nude mice of specific-pathogen-free grade were selected as experimental animals and randomly divided into 2 groups. Then, 10×10^5 RKO cells transfected with SLC2A3 empty vector and with SLC2A3-overexpressed vector were resuspended in 100 μL PBS solution, respectively. Tumor cells were injected through the tail vein using 25-gauge needles. Sixty days later, all mice were euthanized, and bilateral lung tissues were isolated and immediately fixed in a 10% neutral formalin solution for at least 48 hours, and the number of metastatic nodules in the lung tissue was photographed and recorded. Subsequently, the lung tissue was embedded in paraffin for hematoxylin and eosin (H&E) staining and immunohistochemical (IHC) staining. The animal experiments in this study were approved by the Animal Ethics Committee of the Second Affiliated Hospital of Zhejiang University School of Medicine.

2.12 Hematoxylin and eosin (H&E) staining

Representative formalin-fixed, paraffin-embedded lung tissue sections were subjected to H&E staining. In brief, the sections were dewaxed in xylenes for 10 minutes, and then sequentially immersed in 100%, 100%, 95%, 75%, and 50% gradient ethanol for 5 minutes, respectively. After that, the sections were stained with hematoxylin solution for 5 minutes and immersed in 10% eosin solution for 3 minutes. Then, the sections were sequentially immersed in 80% alcohol for 2 minutes, 90% alcohol for 5 minutes, and 100% ethanol for 1 minute. Subsequently, the dehydrated sections were submerged in xylene for 5 minutes twice before being sealed with neutral resin. Finally, the sections were observed under a microscope.

2.13 Immunohistochemistry (IHC)

All surgical specimens, after separation, were fixed within 30 minutes in 10% neutral formalin for at least 24 hours and were routinely dehydrated, paraffin-embedded, and sectioned continuously with a thickness of 4 μm. Then, the two pathologists evaluated hematoxylin and eosin (H&E) staining with double-blind methods. Representative sections were selected for IHC, and all antibodies were processed using the envision two-step method. The experiments were conducted, strictly following the reagent instructions, and completed by the Ventana automatic immunohistochemical system. PBS was used as the negative control instead of the primary antibody, and known positive samples were used as the positive control. The primary antibodies were used as follows: SLC2A3 (1:1000 dilution, proteintech, Cat# 20403-1-AP), YAP-1 (1:500 dilution, Abcam, Cat# EPR19812), and PDGFB (1:100 dilution, Affinity Bioscience, Cat# AF0240). A positive response to all markers was judged as brown or brown-black. Immunohistochemical staining score, based on staining intensity and percentage of stained cells, was calculated as in previous studies (Kuo et al. 2019; Gao et al. 2021) and classified into low (score = 0–2) and high levels (score ≧ 3).

2.14 Statistical analysis

Statistical analysis was conducted using GraphPad Prism 8.0 (GraphPad, Software, San Diego, CA, US) and SPSS 27.0 (SPSS Inc., Chicago, IL, US). All experiments were performed at least three times. The differences between the two groups were analyzed with a two-tailed Chi-square test and a one-way ANOVA analysis was used to analyze more than two groups. The correlation between SLC2A3, YAP-1, and PDGFB expression was calculated using Spearman's rho model. Overall survival was determined using a Kaplan–Meier analysis. The patients' survival comparison was calculated with the log-rank test. $P < 0.05$ was considered statistically significant (*: $P < 0.05$; **: $P < 0.01$; ***: $P < 0.001$).

3 Results

3.1 Aberrant high SLC2A3 expression links to CRC adverse outcomes and overexpression of SLC2A3 accelerates CRC migration and invasion

Firstly, we comprehensively analyzed the mRNA expression profile between CRC tumors and matched

Unedited

normal tissues from the TCGA data. The results showed that SLC2A3 expressions were significantly higher in tumor tissues than in matched normal tissues (Fig. 1A). In addition, the similar findings were consolidated from the GSE68468, GSE44861, GSE44076, and GSE21510 cohorts (Fig. 1B). Therefore, we wondered whether SLC2A3 expression in the tumor affects patient prognosis. Further results showed that high SLC2A3 expression had poorer overall survival than low expression in tumor tissues in TCGA (Fig. 1C), GSE17536 (Fig. 1D), and GSE38832 (Fig. 1E) databases. Thus, we confirmed that SLC2A3 was frequently up-regulated in CRC tissues and was associated with poor prognosis.

To investigate the functions of SLC2A3 in CRC, we detected its expression in CRC cells, including DLD1, RKO, HCT8, SW620, and HCT116 cell lines, at protein and mRNA levels, using Western blotting and RT-PCR methods, respectively. The results revealed that RKO had the lowest SLC2A3 expression and HCT116 had the highest expression among CRC cell lines at the protein level (Fig. 1F). Similarly, its expression is lower in RKO cells than in HCT116 cells at the mRNA level, according to RT-qPCR (Fig. 1G). Subsequently, to explore the role of SLC2A3 in regulating CRC migration and invasion, we transferred siRNA-357 and siRNA-578 to silence SLC2A3 in HCT116 cells, respectively. The Western blotting results showed that siRNA-578 rather than siRNA-357 remarkably down-regulated SLC2A3 protein expression (Fig. 1H), and the knockdown of SLC2A3 in HCT116 cells by specific siRNA-578 dramatically inhibited the capability of migration and invasion in vitro (Figs. 1I-1J). Additionally, we stably knocked down SLC2A3 expression by transferring the SLC2A3-targeted CRISPR-Cas9 vector to HCT116 cells (Fig. 1K). Since SLC2A3 mainly expresses at the cell membrane, we examined the subcellular distribution of SLC2A3 using immunofluorescence assay. As shown in Figure 1L, SLC2A3 located on the cell membrane was significantly reduced in SLC2A3-knocked HCT116 cells compared with the mock control cells. In addition, the results showed that the down-regulation of SLC2A3 also sharply attenuated migration and invasion capacity compared with mock control cells (Figs. 1M-1N); this was consistent with the results of siRNA in HCT116 cells. Furthermore, we used stable overexpression plasmids to over-express Flag-SLC2A3 or empty vector in RKO cells, respectively (Fig. 1O). The results revealed that SLC2A3 located on the cell membrane apparently increased in SLC2A3-overexpressed RKO cells compared with cells treated with empty vector (Fig. 1P), and the overexpression of SLC2A3 markedly enhanced the ability of the cells to migrate and invade in RKO cells (Figs. 1Q-1R).

Taken together, these data confirmed that SLC2A3 prominently promotes CRC cell migration and invasion in vitro.

Unedited

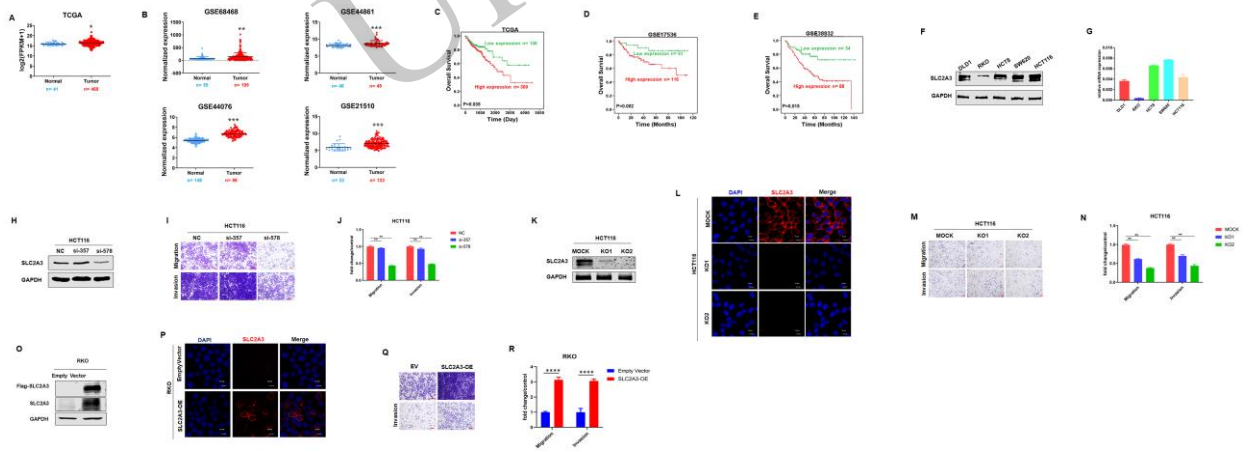

Fig. 1. High expression of SLC2A3 is linked to adverse CRC outcomes and promotes CRC cells' migration and invasion. (A) mRNA expression profile between CRC tumors and matched normal tissues from the TCGA data. (B) mRNA expression profile between CRC tumors and matched normal tissues from the GSE68468, GSE44861, GSE44076, and GSE21510 cohorts. (C-E) High SLC2A3 expression had poorer overall survival than low expression in tumor tissues in TCGA (C), GSE17536 (D), and GSE38832 (E) databases. (F) Western blotting analysis of SLC2A3 protein expression in CRC DLD1, RKO, HCT8, SW620, and HCT116 cell lines. (G) qRT-PCR analysis of SLC2A3 mRNA expression in CRC cell lines. (H) Western blotting analysis of SLC2A3 protein expression in HCT116 cells by transferring siRNA-357 and siRNA-578. (I) Knockdown of SLC2A3 in HCT116 cells by specific siRNA-578 dramatically inhibited the capability for migration and invasion in vitro. (G) Statistical analysis of migration and invasion in SLC2A3-knockdown HCT116 cells by transferring specific siRNA-578. (K) Western blotting analysis of SLC2A3 expression by transferring the SLC2A3-targeted CRISPR-Cas9 vector to HCT116 cells. (L) Examination of the subcellular distribution of SLC2A3 in SLC2A3-KO

HCT116 cells by immunofluorescence assay. (M) Down-regulation of SLC2A3 in SLC2A3-KO HCT116 cells sharply attenuated migration and invasion capacity compared with mock control cells. (N) Statistical analysis of migration and invasion in SLC2A3-KO HCT116 cells. (O) Western blotting analysis of SLC2A3 expression by transferring overexpressed Flag-SLC2A3 or empty vector in RKO cells. (P) Subcellular distribution of SLC2A3 in SLC2A3-overexpressed RKO cells by immunofluorescence assay. (Q) Overexpression of SLC2A3 markedly enhanced the ability of the cells to migrate and invade in RKO cells. (R) Statistical analysis of migration and invasion in SLC2A3-overexpressed RKO cells. Data were analyzed using an unpaired t-test and are presented as mean ± SD in Figure 1 A, B, J, N, R. Kaplan–Meier analysis was applied in Figure 1C-E. EV, empty vector; OE, overexpressed vector; KO, knockout; NC, negative control; si, small interfering; $^{*}P < 0.05$; $^{**}P < 0.01$; $^{***}P < 0.001$.

3.2 SLC2A3 positively regulates YAP-1 and PDGFB expression

To further elucidate the molecular biomechanisms by which SLC2A3 enhances colorectal cancer cell migration and invasion, we performed a genome-wide transcriptional analysis in HCT116 SLC2A3-KO cell lines using RNA sequencing (RNA-seq). Via gene ontology (GO) enrichment analysis based on online tools in the Database for Annotation, Visualization, and Integrated Discovery (DAVID), the top differentially expressed genes (DEGs) were enriched in pathways associated with cancer and cytokine–cytokine receptor interaction (Fig. 2A). Then, we found that cytokine PDGFB expression was dramatically reduced in SLC2A3-knocked HCT116 cells compared with mock control cells (Fig. 2B). As YAP-1, an oncogene involved in the Hippo pathway, promotes glucose and lactate metabolism, it results in the uncontrolled growth and survival of CRC cells (Wang et al. 2015), and may act as a direct target of SLC2A3 to enhance the capacity of cancer cell invasion and lung metastasis (Kuo et al. 2019). So, we simultaneously detected mRNA expression changes in YAP-1 and PDGFB in SLC2A3-knocked HCT116 cells using the qRT-PCR assay. The results showed that down-regulation of SLC3A3 contributed to the remarkably reduced expression of YAP-1 and PDGFB (Figs. 2C-2D). It was a different scenario that in SLC2A3-overexpressed RKO cells (Fig. 2E), up-regulated SLC2A3 resulted in increased expression of YAP-1 and PDGFB (Figs. 2F-2G). The same results were further confirmed by Western blotting assay at protein levels (Figs. 2H-2I). Collectively, we found that SLC2A3 positively regulated YAP-1 and PDGFB expression in CRC cells.

Unedited

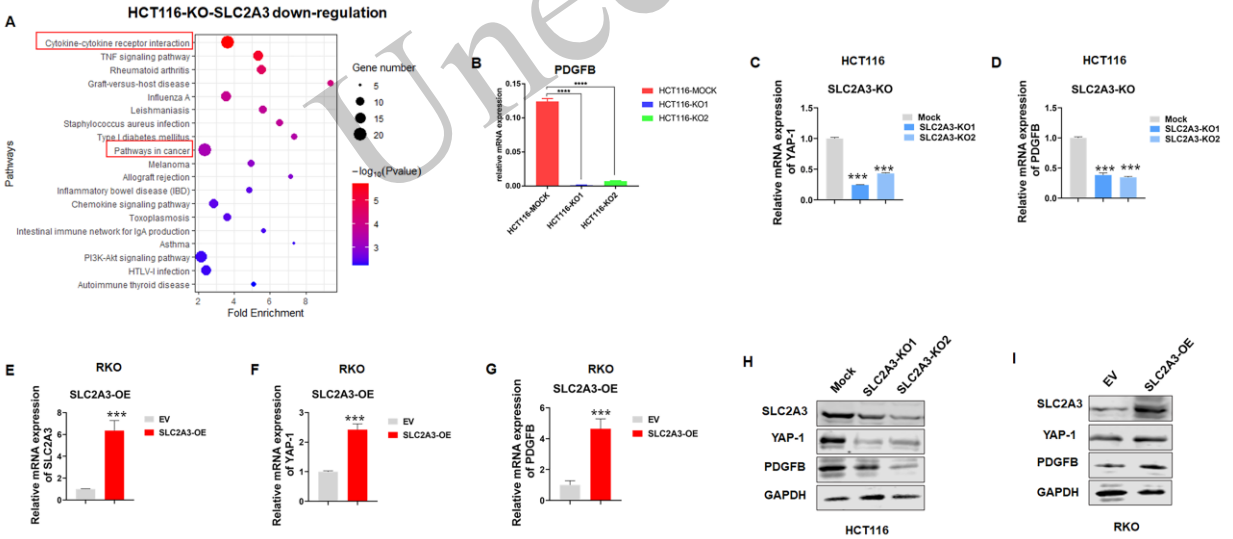

Fig. 2. SLC2A3 positively regulates YAP-1 and PDGFB expression. (A) A genome-wide transcriptional analysis and pathway enrichment analysis were performed in HCT116 SLC2A3-KO cell lines using RNA-seq. (B) Cytokine PDGFB expression was analyzed by qRT-PCR in SLC2A3-KO HCT116 cells using RNA-seq. (C, D) mRNA expression of YAP-1 (C) and PDGFB (D) in SLC2A3-KO HCT116 cells by qRT-PCR assay. (E) qRT-PCR analysis of SLC2A3 mRNA expression in SLC2A3-overexpressed RKO cells. (F, G) qRT-PCR analysis of mRNA expression of YAP-1 (F) and PDGFB (G) in SLC2A3-overexpressed RKO cells. (H) Western blotting analysis of YAP-1 protein expression in SLC2A3-KO HCT116 cells. (I) Western blotting analysis of PDGFB protein expression in SLC2A3-overexpressed RKO cells. Data were analyzed using an unpaired t-test and are presented as mean ± SD in Figure 2B-G. RNA-seq, RNA sequencing; EV, empty vector; OE, overexpressed vector; KO, knockout; ***P < 0.001.

3.3 SLC2A3 up-regulates PDGFB expression via simulating YAP-1

To further illuminate the molecular mechanism by which SLC2A3 regulates YAP-1 and PDGFB expression, we re-expressed SLC2A3 into SLC2A3-KO HCT116 cells. Intriguingly, at transcriptional levels, SLC2A3 overexpression significantly rescued YAP-1 and PDGFB mRNA expression detected by qRT-PCT (Figs. 3A-3D). Instead, as we knocked down SLC2A3 expression by retransferring siSLC2A3-578 in SLC2A3-overexpressed RKO cells (Figs. 3F-3G), YAP-1 and PDGFB mRNA expression markedly dropped (Figure 3H-K). Similar protein level results were also validated in HCT116 and RKO cells (Figs. 3E-3L). Therefore, these results further reinforce that SLC2A3 positively regulates YAP-1 and PDGFB expression in CRC cells. Recent studies have indicated that YAP-1 might transcriptionally up-regulate downstream cofactors like PDGFB to facilitate tumor malignant progression in bladder cancer and nasopharyngeal carcinoma (Wang et al. 2019; Liang et al. 2020). To explore whether SLC2A3 regulates PDGFB expression through YAP-1 or vice versa, we knocked down YAP-1 expression by transfecting siRNA in SLC2A3-overexpressed RKO cells (Figure 3M). Interestingly, the results showed that YAP-1 downexpression sharply reduced PDGFB expression at both mRNA and protein levels (Figs. 3N-3O). Therefore, we conclude that SLC2A3 up-regulates PDGFB expression by activating YAP-1.

Unedited

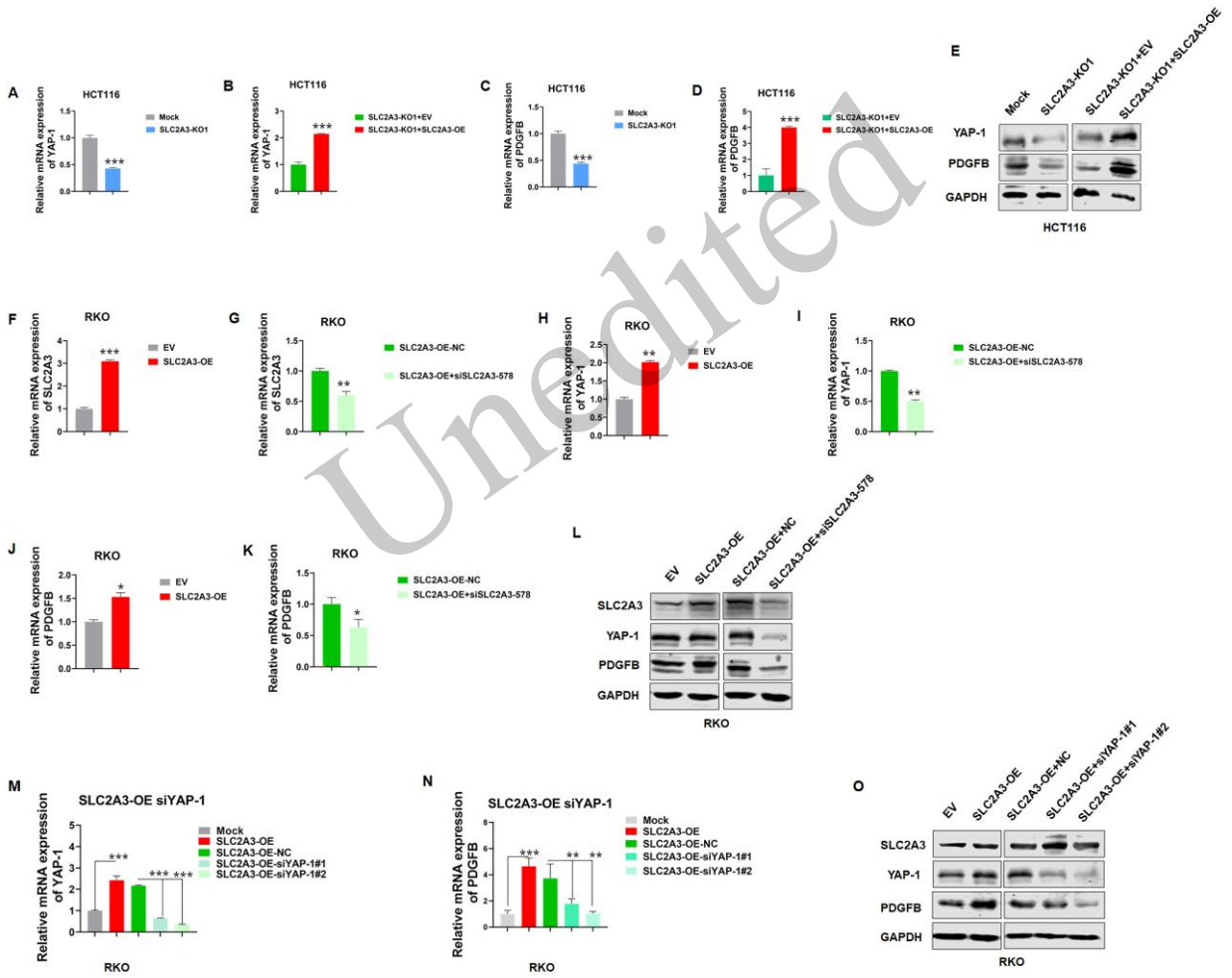

Fig. 3. SLC2A3 up-regulates PDGFB expression via simulating YAP-1. (A) qRT-PCR analysis of YAP-1 mRNA expression in SLC2A3-KO HCT116 cell. (B) SLC2A3 overexpression significantly rescued YAP-1 mRNA expression in SLC2A3-KO HCT116 cell. (C) qRT-PCR analysis of PDGFB mRNA expression in SLC2A3-KO HCT116 cell. (D) SLC2A3 overexpression significantly rescued PDGFB mRNA expression in SLC2A3-KO HCT116 cell. (E) Western blotting analysis of YAP-1 and PDGFB protein expression in SLC2A3-KO HCT116 cells and SLC2A3-KO plus SLC2A3 OE HCT116 cells. (F) qRT-PCR analysis of SLC2A3 mRNA expression in SLC2A3-overexpressed RKO cell. (G) qRT-PCR analysis of SLC2A3 expression in SLC2A3-overexpressed RKO cells by retransferring siSLC2A3-578. (H and I) Detection of YAP-1 expression in SLC2A3-overexpressed RKO cell (H) and SLC2A3-overexpressed RKO cell by retransferring siSLC2A3-578 (I). (J and

K) Detection of PDGFB expression in SLC2A3-overexpressed RKO cell (J) and SLC2A3-overexpressed RKO cell by retransferring siSLC2A3-578 (K). PDGFB mRNA expression in SLC2A3-KO HCT116 cell. (L) YAP-1 and PDGFB expression in SLC2A3-overexpressed RKO cell and SLC2A3-overexpressed RKO cell by retransferring siSLC2A3-578 by Western blotting. (M) Detection of YAP-1 expression by transfecting siRNA in SLC2A3-overexpressed RKO cells. (N and O) YAP-1 downexpression sharply reduced PDGFB expression at both mRNA (N) and protein (O) levels. Data were analyzed using an unpaired t-test and are presented as mean ± SD in Figure 3A-D, F-K, M, and N. EV, empty vector; OE, overexpressed vector; KO, knockout; NC, negative control; si, small interfering; *P < 0.05; **P < 0.01; ***P < 0.001.

3.4 PDGFB promotes CRC cells migration and invasion

To further investigate how SLC2A3 promotes CRC cell migration and invasion through up-regulating PDGFB expression in CRC cells, we transfected an empty vector and a PDGFB overexpressed vector into RKO cells, respectively (Fig. 4A). The results showed that PDGFB overexpression markedly promoted RKO cell migration and invasion measured by transwell assays (Figs. 4B-4C). Furthermore, since PDGFB acts as a cytokine secreted mainly from activated platelets in an autocrine or paracrine manner (Zhang et al. 2020) when treated with increased dosages of PDGFB, from 50ng/ml, 500ng/ml, 5μg/ml, and to 50μg/ml independently. Strikingly, SLC2A3-knocked HCT116 cells exhibited a remarkably increased potential for migration and invasion compared with mock control cells (Figs. 4D-4F). Collectively, these results confirm that PDGFB shows a notable capability to promote CRC cell migration and invasion.

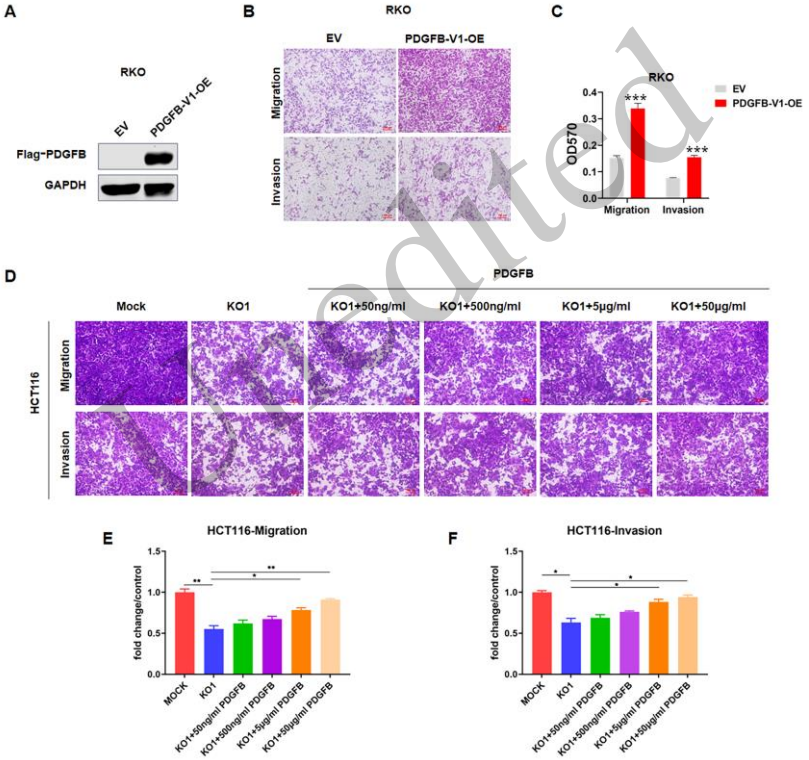

Fig. 4. PDGFB promotes CRC cells' migration and invasion. (A) Detection of PDGFB expression in PDGFB-overexpressed RKO cells by Western blotting. (B) Migration and invasion were analyzed by transwell assays in PDGFB-overexpressed RKO cells. (C) Statistical analysis of migration and invasion in PDGFB-overexpressed RKO cells. (D) Migration and invasion were analyzed by transwell assays in SLC2A3-KO HCT116 cells when treated with increasing dosages of PDGFB, from 50ng/ml, 500ng/ml, 5μg/ml, and to 50μg/ml independently. (E and F) Statistical analysis of migration (E) and invasion (F) when treated with different dosages of PDGFB. Data were analyzed using an unpaired t-test and are presented as mean ± SD in Figure 4C, E, F. EV, empty vector; OE, overexpressed vector; KO, knockout; *P < 0.05; **P < 0.01; ***P < 0.001.

3.5 SLC2A3 promotes lung metastasis of colorectal cancer cells

To further investigate the effect of SLC2A3 on the distant metastasis of colorectal cancer in vivo, we conducted mouse xenograft experiments by injecting RKO cells transfected with SLC2A3 empty vector (as the control group) and with SLC2A3-overexpressed vector (as an experimental group) into the tail veins to assess the formation of lung metastasis. The findings demonstrated that, compared to the control group, the

SLC2A3-overexpressed RKO cell group exhibited a greater number of visible metastatic nodes in the lung tissue (Figs. 5A-B)($P < 0.01$). H&E staining tissue sections also revealed that a few small metastatic nodules scattered in the lung tissue in the control group, whereas a large number of metastatic lesions occupied most of the entire lung tissue in the SLC2A3-overexpressed RKO cell group (Figs. 5C-5D). In addition, the results of the immunohistochemical staining demonstrated that the expression levels of SLC2A3, YAP-1, and PDGFB in the metastatic lesions of the lung tissue in the experimental group were significantly higher compared to the control group (Fig. 5E). Consequently, the in vivo mouse xenograft studies provided additional evidence that SLC2A3 promoted CRC cells' distant lung metastasis by activating the YAP-1/PDGFB axis.

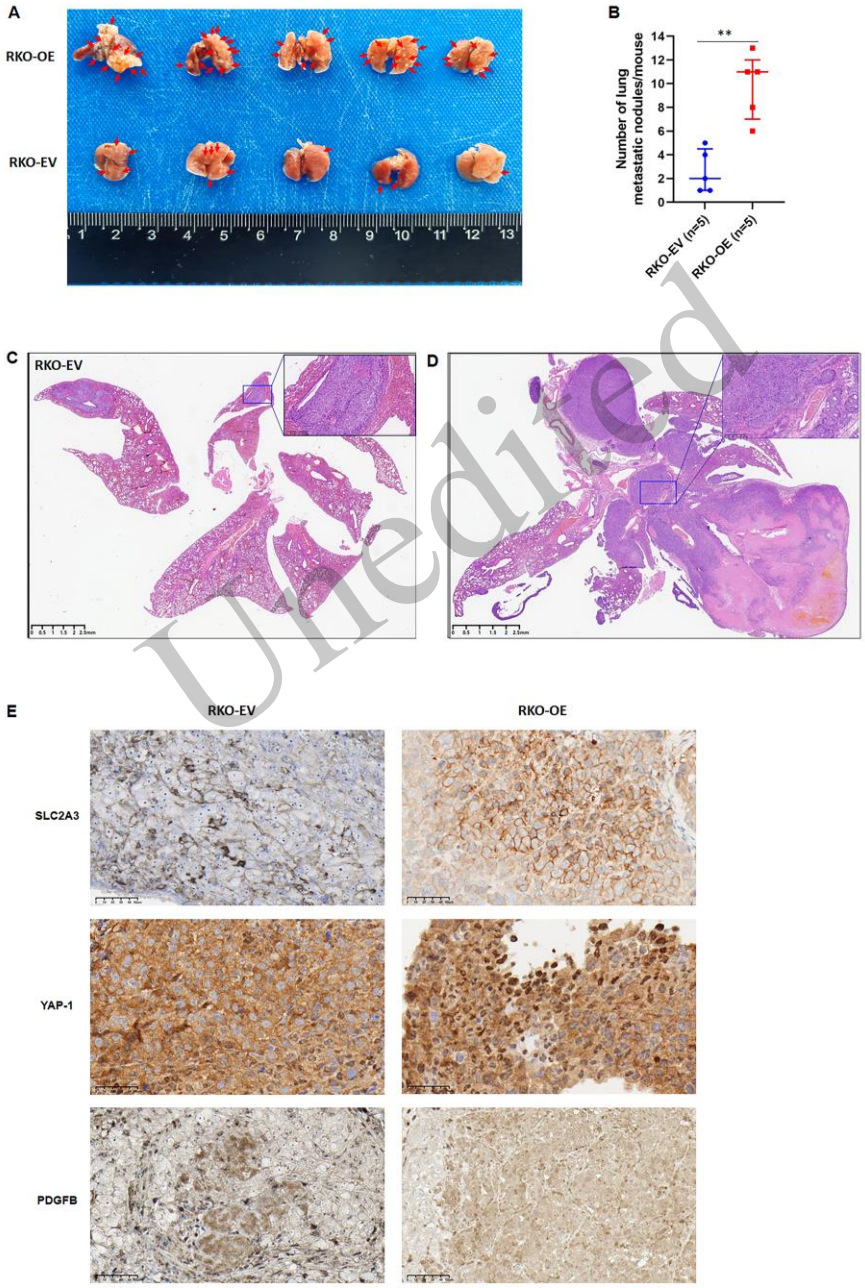

Unedited

Fig. 5. SLC2A3 promoted lung metastasis of colorectal cancer cells in mouse xenograft model. (A, B) The number of metastatic nodes in the lung tissue in the control group that the RKO cells transfected with SLC2A3 empty vector and group transfected with SLC2A3-overexpressed vector. (C, D) Representative H&E staining section of metastatic nodules

in the lung tissue in the control group and the SLC2A3-overexpressed RKO cell group. (E) Representative IHC staining of SLC2A3, YAP-1, and PDGFB expression in the metastatic nodules of the lung tissue in the SLC2A3 empty vector group and SLC2A3-overexpressed RKO cell group. Data were analyzed using an unpaired t-test and are presented as mean ± SD in Figure 5B. H&E, Hematoxylin and eosin staining; IHC, immunohistochemical staining; EV, empty vector; OE, over-expressed vector; →, metastatic nodules; **P < 0.01.

3.6 Relationships between SLC2A3, YAP-1, and PDGFB protein expression and clinicopathological features

To gain insight into the relationship between SLC2A3, YAP-1, and PDGFB protein expression and clinicopathological factors, we examined SLC2A3, YAP-1, and PDGFB expression levels in formalin-fixed paraffin-embedded 135 CRC surgical tissues by immunohistochemistry. Tumor samples assessed by immunohistochemistry were scored based on stain intensity and extent (Figs. 6A-6L). Next, the patients were classified into SLC2A3-low (n=86) and SLC2A3-high (n=49), YAP-1-low (n=94) and YAP-1-high (n=41), and PDGFB-low (n=96) and PDGFB-high (n=39) expression groups, respectively. The results revealed that increased SLC2A3, YAP-1, and PDGFB expression were remarkably associated with lymph node metastasis ($P < 0.001$, $P = 0.016$, $P < 0.001$), nervous invasion ($P < 0.001$, $P = 0.001$, $P < 0.001$), lymphovascular invasion ($P < 0.001$, $P = 0.007$, $P < 0.001$), distant metastasis ($P < 0.001$, $P < 0.001$, $P < 0.001$), and pTNM stage ($P < 0.001$, $P = 0.001$, $P < 0.001$), respectively. In addition, there was a slight association between increased YAP-1 expression and pT stage ($P = 0.048$). There were no significant differences between these protein expressions and other tumor-related factors, such as gender, age, tumor location, tumor size, gross subgroup, or histological classification (Table 1).

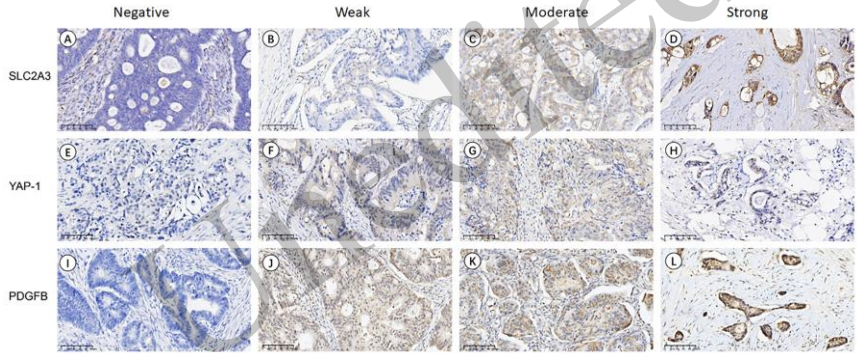

Fig. 6. Representative immunohistochemical staining of SLC2A3, YAP-1, and PDGFB in CRC.
SLC2A3 expression negative (A), weak (B), moderate (C), strong (D); YAP-1 expression negative (E), weak (F), moderate (G), strong (H); PDGFB expression negative (I), weak (J), moderate (K), strong (L). Bar: 100 μm, 200x.

Table 1. Clinicopathological characteristics of SLC2A3, YAP-1, and PDGFB expression in CRC patients.

Parameters	SLC2A3 expression		*P* value	YAP-1 expression		*P* value	PDGFB expression		*P* value
	Low n=86(%)	High n=49(%)		Low n=94(%)	High n=41(%)		Low n=96(%)	High n=39(%)	
Gender			0.246			0.503			0.308
Male	51(37.80)	24(17.80)		54(40.00)	21(15.60)		56(41.50)	19(14.10)	
Female	35(25.90)	25(18.50)		40(29.40)	20(14.80)		40(29.40)	20(14.80)	
Age (Years)			0.757			0.579			0.885
≤60	38(28.10)	23(17.00)		41(30.40)	20(14.80)		43(31.90)	18(13.30)	
> 60	48(35.60)	26(19.30)		53(39.30)	21(15.60)		53(39.30)	21(15.60)	
Tumor location			0.402			0.308			0.330
Colon	52(38.50)	26(19.30)		57(42.20)	21(15.60)		58(43.00)	20(14.80)	
Rectum	34(25.20)	23(17.00)		37(27.40)	20(14.80)		38(28.10)	19(14.10)	
Tumor size (cm)			0.441			0.579			0.885
≤5	45(33.30)	29(21.50)		53(39.30)	21(15.60)		53(39.30)	21(15.60)	

> 5	41(30.40)	20(14.80)		41(30.40)	20(14.80)		43(31.90)	18(13.30)	
Gross subgroup			0.850			0.565			0.917
Ulcerative	53(39.30)	31(23.00)		57(42.20)	27(20.00)		60(44.40)	24(17.80)	
others	33(24.40)	18(13.30)		37(27.40)	14(10.40)		36(26.70)	15(11.10)	
Histological classification			0.720			0.134			0.184
Tubular	68(50.40)	40(29.40)		72(53.30)	36(26.70)		74(54.80)	34(25.20)	
others	18(13.30)	9(6.70)		22(16.30)	5(3.70)		22(16.30)	5(3.70)	
Differentiation			0.670			0.834			0.517
Well/Moderate	66(48.90)	36(26.70)		72(53.30)	30(22.20)		74(54.80)	28(20.70)	
Poor	20(14.80)	13(9.60)		22(16.30)	11(8.10)		22(16.30)	11(8.10)	
pT stage			0.055			**0.048**			0.075
0/1/2	27(20.00)	8(5.90)		29(21.50)	6(4.40)		29(21.50)	6(4.40)	
3/4	59(43.70)	41(30.40)		65(48.10)	35(25.90)		67(49.60)	33(24.40)	
Lymph node metastasis			**<0.001**			**0.016**			**<0.001**
Negative	59(43.70)	18(13.30)		60(44.40)	17(12.60)		65(48.10)	12(8.90)	
Positive	27(20.00)	31(23.00)		34(25.20)	24(17.80)		31(23.00)	27(20.00)	
Nervous invasion			**<0.001**			**0.001**			**<0.001**
Negative	79(58.50)	27(20.00)		81(60.00)	25(18.50)		84(62.20)	22(16.30)	
Positive	7(5.20)	22(16.30)		13(9.60)	16(11.90)		12(8.90)	17(12.60)	
Lymphovascular invasion			**<0.001**			**0.007**			**<0.001**
Negative	57(42.20)	13(9.60)		56(41.50)	14(10.40)		60(44.40)	10(7.40)	
Positive	29(21.50)	36(26.70)		38(28.10)	27(20.00)		36(26.70)	29(21.50)	
Distant metastasis			**<0.001**			**<0.001**			**<0.001**
M0	86(63.70)	32(23.70)		92(68.10)	26(19.30)		96(71.10)	22(16.30)	
M1	0(0.00)	17(12.60)		2(1.50)	15(11.10)		0(0.00)	17(12.60)	
pTNM stage			**<0.001**			**0.001**			**<0.001**
I/II	57(42.20)	14(10.40)		58(43.00)	13(9.60)		63(46.70)	8(5.90)	
III/IV	29(21.50)	35(25.90)		36(26.70)	28(20.70)		33(24.40)	31(23.00)	

Data were analyzed using an unpaired t test.

Unedited

3.7 Correlation analyses and prognostic value of SLC2A3, YAP-1, and PDGFB expression in CRC

To investigate the correlation between SLC2A3, YAP-1, and PDGFB expression in our immunohistochemical cohort and TCGA data, Spearman's rho model was performed. The results showed that the expressions between SLC2A3 and YAP-1 were positively correlated (R = 0.44, $P < 0.001$) (Fig. 7A). SLC2A3 expression likewise has a significant positive correlation with PDGFB expression (R = 0.49, $P < 0.001$) (Fig. 7B). Additionally, YAP-1 expression was positively correlated with PDGFB expression (R = 0.56, $P < 0.001$) (Fig. 7C). Additionally, these results were further confirmed at the mRNA level in TCGA data, and there was a positive correlation between SLC2A3 and YAP-1 (R = 0.23, $P < 0.001$) (Fig. 7D), SLC2A3 and PDGFB (R = 0.70, $P < 0.001$) (Fig. 7E), and YAP-1 and PDGFB (R = 0.18, $P = 0.0004$) (Fig. 7F), respectively. As a result, we demonstrated a significant positive correlation between the three proteins.

Next, the Kaplan–Meier analysis was applied by log-rank test to assess the prognostic significance of SLC2A3, YAP-1, and PDGFB expression in our immunohistochemical cohort and TCGA data. The results from our cohort showed that patients with high expression of SLC2A3, YAP-1, and PDGFB protein had strikingly

shorter overall survival compared with those with low expression ($P < 0.001$, $P = 0.001$, $P < 0.001$, respectively) (Figs. 7G-7I). Moreover, we analyzed TCGA data and confirmed that YAP-1 and PDGFB mRNA expressions were significantly higher in tumor tissues than in matched normal tissues (Figs. 7J-7K), respectively, and their high expression showed a similar tendency to poor outcomes, as demonstrated in our cohort (Figs. 7L-7M). Therefore, we conclude that increased SLC2A3, YAP-1, and PDGFB expression was an adverse prognostic factor for CRC patients.

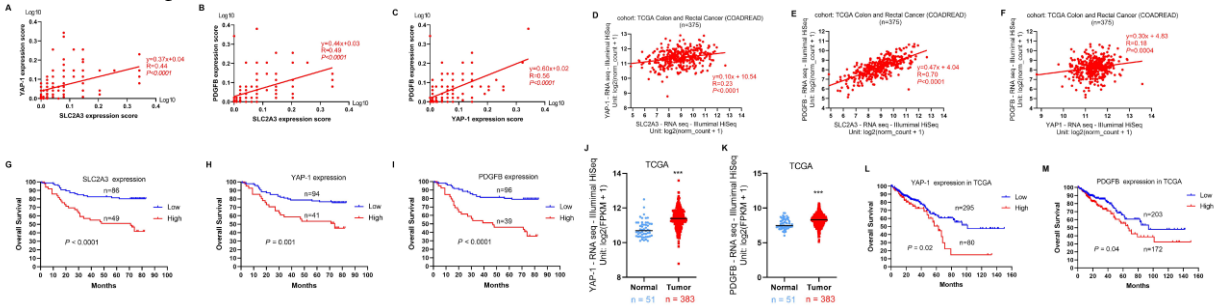

Fig. 7. SLC2A3, YAP-1, and PDGFB expressions had a significant positive correlation with each other in our cohort and TCGA data, and increased SLC2A3, YAP-1, and PDGFB expression was an adverse prognostic factor for CRC patients in our cohort and TCGA data. (A-C) Correlation analyses by Spearman's rho model showed that SLC2A3 and YAP-1 (A), SLC2A3 and PDGFB (B), and YAP-1 and PDGFB (C) were positively correlated in our cohort. The positive correlations were also confirmed by TCGA data (D-F). (G-I) Kaplan–Meier analysis was applied to assess the prognostic significance between SLC2A3 (G), YAP-1 (H), and PDGFB (I) expression in our cohort. (J-K) YAP-1 (J), and PDGFB (K) mRNA expressions were analyzed in TCGA data. (L-M) Survival significance of YAP-1 (L) and PDGFB (M) expressions with Kaplan–Meier analysis in TCGA data. Data were analyzed using an unpaired t-test and are presented as mean ± SD in Figure 7J, K. ***P < 0.001.

Unedited

4 Discussion

Recently, numerous investigations have revealed that several members of the glucose transporter family participate in the tumor malignant process by regulating aerobic glycolysis; for example, SLC2A1 and SLC2A12 serve as an oncogene and are associated with tumor malignant transformation, aggressive behaviors, and poor prognosis in breast cancer (Wellberg et al. 2016; Shi et al. 2020), and SLC2A14 may partially be responsible for predicting the therapeutic effects of anti-PD-1 on melanoma (Triozzi et al. 2022). An overwhelming number of studies have focused on the pivotal roles of SLC2A3 in the aerobic glycolysis metabolism process to regulate tumor progression in response to an adverse tumor microenvironment. Warburg effects, a well-known universal phenomenon whereby glucose is reprogrammed to undergo an aerobic glycolysis metabolism process in the absence or even presence of nutrients or oxygen in various neoplasm cells, can provide a steady energy stream for tumor self-refreshment, malignant transforming, proliferation, aggression, distant metastasis, and drug resistance (Liberti and Locasale 2016; Lu 2019; Hosios and Manning 2021). These studies suggested that aberrantly increased SLC2A3 expression plays a crucial role in tumor progression by participating in various signaling pathways mainly involving Warburg effects, such as the PI3K/AKT, MAPK, and IKKα/IKKβ/NFκB pathways, thus protecting tumor cell survival from threats and accelerating malignant aggression (Kawauchi et al. 2008; Tahir et al. 2013; Barron et al. 2016; Chen et al. 2018; Hosios and Manning 2021). Correspondingly, interrupting these pathways by inhibiting SLC2A3 may be a practicable strategy for tumor treatment (Hsieh et al. 2014). Whereas, up to now, the underlying regulatory mechanisms of non-glycolytic pathways by which SLC2A3 boosts tumor progression have not been fully unearthed, in this paper, we elucidate that SLC2A3 is commonly up-regulated in CRC and is associated with poor prognosis. More intriguingly, SLC2A3 enhances CRC migration, invasion, and distant lung metastasis by activating the YAP-1/PDGFB axis.

In this study, systematic data analysis indicated that SLC2A3 was significantly up-regulated in CRC tissues compared to normal tissues and may be an indicator of poor CRC prognosis, which is consistent with previous research on CRC (Martinez-Romero et al. 2018; Kim et al. 2019; Wu et al. 2020; Gao et al. 2021). Mechanistically, previous studies have confirmed that, in response to hypoxia or nutrient depletion, nuclear oncogene CREB1, CDK8, and Caveolin-1 (Cav-1) positively regulated SLC2A3, of which CREB1 could per-

tinently up-regulate SLC2A3 expression, while Cav-1 increased SLC2A3 expression through directly binding and interacting with high mobility group protein A1 (HMGA1) and SLC2A3 promoter regions. Meanwhile, HMGA1 may directly bind with SLC2A3, and SLC2A3, in turn, boosts HMGA1-induced CRC distant liver metastasis. The ultimate interaction therefore resulted in continuous glucose uptake and aerobic glycolysis for uncontrolled tumor growth and malignant progression (Ha and Chi 2012; Ha et al. 2012; Galbraith et al. 2017; Yang et al. 2020). Intriguingly, in this study, we analyzed gene set pathway enrichment using RNA next-generation sequencing technology in SLC2A3-knocked HCT116 cells, and the results revealed that SLC2A3 most frequently affected pathways associated with cancer and cytokine–cytokine receptor interaction. We also found that YAP-1 and cytokine PDGFB expressions were dramatically reduced in SLC2A3-knocked HCT116 cells. These data indicate that SLC2A3 might partially promote CRC migration and invasion by regulating YAP-1 and PDGFB expression, which offers a novel perspective on the biomechanisms underlying SLC2A3's regulation of CRC aggression.

In addition to this, one study showed that the activation of the fibronectin-induced integrin αvβ1/ FAK/cell division cycle 42 (CDC42) signaling pathway up-regulated SOX2 expression by simulating YAP-1, thus facilitating CRC cell proliferation and drug resistance (Ye et al. 2020). Furthermore, other studies have confirmed that the activation of YAP-1 directly targeted and up-regulated SLC2A3 expression; in turn, elevated SLC2A3 expression directly activated and up-regulated YAP-1 expression, thereby forming a positive SLC2A3-YAP-1 feedback loop, enhancing glucose metabolism to promote cancer cells' proliferation, migration, invasion, and lung metastasis (Wang et al. 2015; Kuo et al. 2019; Jiang et al. 2021). In line with these results, we also revealed that SLC2A3 could positively regulate YAP-1 and PDGFB expression.

PDGFB was first detected in the tissue specimens of CRC patients (Ito et al. 1990). Later, some researchers documented that the plasma-secreted PDGFBB level was significantly higher in CRC than in adenoma (Belizon et al. 2009) and was associated with advanced CRC and adverse prognosis by recruiting pericytes and enhancing angiogenesis, which makes it a potential biomarker for the early diagnosis of CRC (McCarty et al. 2007; Nakamura et al. 2008; Ionescu et al. 2011). Considering PDGFBB as a major interactor with PDGFR-ββ, blocking the PDGFBB/PDGFR-ββ signaling pathway resulted in effective abrogation of cancer cell proliferation and distant metastasis (Shan et al. 2011). However, other investigations emphasized that drugs targeting PDGF may be counterproductive when there are low levels of PDGFBB in the microenvironment due to the decreasing pericyte numbers for facilitating the tumor cells' proliferation and metastasis (Hosaka et al. 2013). Another study showed that, in pancreatic cancer, high PDGFBB expression promoted tumor cell proliferation and migration by simulating the YAP-related Hippo pathway (Li et al. 2021). On the contrary, in the present study, we demonstrated that SLC2A3 positively regulated YAP-1 expression, and PDGFB acted as a crucial downstream molecule of YAP-1. We also confirmed that overexpression of PDGFB within tumor cells or increased concentrations of PDGFB agents in the tumor microenvironment markedly enhanced CRC migration and invasion. In summary, the results of the present study indicate that the relationship among SLC2A3, YAP-1, and PDGFB may be intricate, and there may be a positive feedback loop among them. Thus, the underlying mechanisms need to be deeply excavated.

We confirmed that high SLC2A3, YAP-1, and PDGFB expressions in CRC tissues were significantly correlated with lymph node metastasis, nervous invasion, lymphovascular invasion, distant metastasis, and pTNM stage, respectively. We also further found that there was a correlation with the expression of SLC2A3, YAP-1, and PDGFB in CRC tissues, and their high expressions were hazard factors for CRC, which is consistent with the findings of previous studies (Nakamura et al. 2008; Sun et al. 2019; Wu et al. 2020; Gao et al. 2021; Yao et al. 2022). Although Yoshito Nakamura and colleagues confirmed that high PDGFBB expression was only associated with vascular invasion rather than other clinicopathological factors, they also documented that high PDGFBB expression was an independent risk factor for CRC (Nakamura et al. 2008). Nevertheless, in our study, we confirmed that high PDGFB protein expression in CRC tissues was linked to lymphovascular invasion, lymph node metastasis, nervous invasion, distant metastasis, and pTNM stage. Furthermore, our findings corroborated that SLC2A3 enhanced CRC malignant aggression and was associated with poor prognosis by activating the YAP-1/PDGFB axis.

Uncorrected

5 Conclusions

In this study, we initially demonstrated that SLC2A3 acts as an oncogene to enhance CRC cell malignant aggression and is linked to poor outcomes by positively activating the YAP-1/PDGFB axis. This not only expands the understanding of the biomechanisms by which SLC2A3 promotes CRC aggression but also offers a novel tool for CRC targeted therapy. Moreover, the present results also indicate that there may be crosstalk between the SLC2A3-regulated YAP-1/PDGFB axis, the YAP-related Hippo signaling pathway, and PDGFBB/PDGFR-ββ signaling pathway, and there may be positive feedback regulation among these signaling pathways. Thus, methods to interrupt these signaling pathways, including directly targeting SLC2A3, may be feasible for CRC treatment, especially for reversing resistance and preventing or blocking CRC distant metastasis (Cao et al. 2007; Karageorgis et al. 2018; Ceballos et al. 2019; Reckzeh et al. 2019). Therefore, all the above issues will be investigated and deciphered in future work.

Data availability statement

The datasets used and/or analyzed during the current study are available from the authors upon reasonable request.

Acknowledgments

This research is supported by the National Natural Science Foundation of China (No. 82072624).

Authors' contributions

Kefeng DING designed and supervised the project. Jinlong TANG interpreted the results and drafted and improved the main manuscript. Jinlong TANG, Mailang MAI, and Fengyan HAN performed all experiments. Chaoyi CHEN and Shuli XIA contributed to the statistical analyses. Qi YANG and Xueping XIANG performed immunohistochemistry. All authors read and approved the final manuscript.

Compliance with ethics guidelines

Jinlong TANG, Mailang MAI, Fengyan HAN, Chaoyi CHEN, Shuli XIA, Qi YANG and Xueping XIANG, and Kefeng DING declare that they have no conflict of interest.

The research is approved by the human research ethical committee of the Second Affiliated Hospital, Zhejiang University School of Medicine, and the ethical approval number is No.2022-0735, and the animal experiments in this study were approved by the Animal Ethics Committee of the Second Affiliated Hospital of Zhejiang University School of Medicine (No: 2023-091).

Unedited

References

Akervall J, Nandalur S, Zhang J, et al. 2014. A novel panel of biomarkers predicts radioresistance in patients with squamous cell carcinoma of the head and neck. Eur J Cancer 50(3): 570-581. https://doi.org/10.1016/j.ejca.2013.11.007

An Y, Varma VR, Varma S, et al. 2018. Evidence for brain glucose dysregulation in Alzheimer's disease. Alzheimers Dement 14(3): 318-329. https://doi.org/10.1016/j.jalz.2017.09.011

Ayala FR, Rocha RM, Carvalho KC, et al. 2010. GLUT1 and GLUT3 as potential prognostic markers for Oral Squamous Cell Carcinoma. Molecules 15(4): 2374-2387. https://doi.org/10.3390/molecules15042374

Barron CC, Bilan PJ, Tsakiridis T, et al. 2016. Facilitative glucose transporters: Implications for cancer detection, prognosis and treatment. Metabolism 65(2): 124-139. https://doi.org/10.1016/j.metabol.2015.10.007

Belizon A, Balik E, Horst PK, et al. 2009. Platelet-derived growth factor (subtype BB) is elevated in patients with colorectal carcinoma. Dis Colon Rectum 52(6): 1166-1171. https://doi.org/10.1007/DCR.0b013e3181a0b388

Cao X, Fang L, Gibbs S, et al. 2007. Glucose uptake inhibitor sensitizes cancer cells to daunorubicin and overcomes drug resistance in hypoxia. Cancer Chemother Pharmacol 59(4): 495-505. https://doi.org/10.1007/s00280-006-0291-9

Ceballos J, Schwalfenberg M, Karageorgis G, et al. 2019. Synthesis of Indomorphan Pseudo-Natural Product Inhibitors of Glucose Transporters GLUT-1 and -3. Angew Chem Int Ed Engl 58(47): 17016-17025. https://doi.org/10.1002/anie.201909518

Chen D, Wang H, Chen J, et al. 2018. MicroRNA-129-5p Regulates Glycolysis and Cell Proliferation by Targeting the Glucose Transporter SLC2A3 in Gastric Cancer Cells. Front Pharmacol 9: 502. https://doi.org/10.3389/fphar.2018.00502

Cosset E, Ilmjarv S, Dutoit V, et al. 2017. Glut3 Addiction Is a Druggable Vulnerability for a Molecularly Defined Subpopulation of Glioblastoma. Cancer Cell 32(6): 856-868 e855.
https://doi.org/10.1016/j.ccell.2017.10.016

Dubois F, Keller M, Hoflack J, et al. 2019. Role of the YAP-1 Transcriptional Target cIAP2 in the Differential Susceptibility to Chemotherapy of Non-Small-Cell Lung Cancer (NSCLC) Patients with Tumor RASSF1A Gene Methylation from the Phase 3 IFCT-0002 Trial. Cancers (Basel) 11(12).
https://doi.org/10.3390/cancers11121835

Eefsen RL, Van den Eynden GG, Hoyer-Hansen G, et al. 2012. Histopathological growth pattern, proteolysis and angiogenesis in chemonaive patients resected for multiple colorectal liver metastases. J Oncol 2012: 907971.
https://doi.org/10.1155/2012/907971

Fidler TP, Marti A, Gerth K, et al. 2019. Glucose Metabolism Is Required for Platelet Hyperactivation in a Murine Model of Type 1 Diabetes. Diabetes 68(5): 932-938.
https://doi.org/10.2337/db18-0981

Galbraith MD, Andrysik Z, Pandey A, et al. 2017. CDK8 Kinase Activity Promotes Glycolysis. Cell Rep 21(6): 1495-1506.
https://doi.org/10.1016/j.celrep.2017.10.058

Gao H, Liang J, Duan J, et al. 2021. A Prognosis Marker SLC2A3 Correlates With EMT and Immune Signature in Colorectal Cancer. Front Oncol 11: 638099.
https://doi.org/10.3389/fonc.2021.638099

Global Burden of Disease Cancer C, Kocarnik JM, Compton K, et al. 2022. Cancer Incidence, Mortality, Years of Life Lost, Years Lived With Disability, and Disability-Adjusted Life Years for 29 Cancer Groups From 2010 to 2019: A Systematic Analysis for the Global Burden of Disease Study 2019. JAMA Oncol 8(3): 420-444.
https://doi.org/10.1001/jamaoncol.2021.6987

Greenhalgh DG, Sprugel KH, Murray MJ, et al. 1990. PDGF and FGF stimulate wound healing in the genetically diabetic mouse. Am J Pathol 136(6): 1235-1246.

Ha TK and Chi SG 2012. CAV1/caveolin 1 enhances aerobic glycolysis in colon cancer cells via activation of SLC2A3/GLUT3 transcription. Autophagy 8(11): 1684-1685.
https://doi.org/10.4161/auto.21487

Ha TK, Her NG, Lee MG, et al. 2012. Caveolin-1 increases aerobic glycolysis in colorectal cancers by stimulating HMGA1-mediated GLUT3 transcription. Cancer Res 72(16): 4097-4109.
https://doi.org/10.1158/0008-5472.CAN-12-0448

Hosaka K, Yang Y, Seki T, et al. 2013. Tumour PDGF-BB expression levels determine dual effects of anti-PDGF drugs on vascular remodelling and metastasis. Nat Commun 4: 2129.
https://doi.org/10.1038/ncomms3129

Hosios AM and Manning BD 2021. Cancer Signaling Drives Cancer Metabolism: AKT and the Warburg Effect. Cancer Res 81(19): 4896-4898.
https://doi.org/10.1158/0008-5472.CAN-21-2647

Hsieh IS, Yang RS and Fu WM 2014. Osteopontin upregulates the expression of glucose transporters in osteosarcoma cells. PLoS One 9(10): e109550.
https://doi.org/10.1371/journal.pone.0109550

Hsu YL, Yen MC, Chang WA, et al. 2019. CXCL17-derived CD11b(+)Gr-1(+) myeloid-derived suppressor cells contribute to lung metastasis of breast cancer through platelet-derived growth factor-BB. Breast Cancer Res 21(1): 23.
https://doi.org/10.1186/s13058-019-1114-3

Ionescu C, Berindan-Neagoe I, Burz C, et al. 2011. The clinical implications of platelet derived growth factor B, vascular endothelial growth factor and basic fibroblast growth factor in colorectal cancer. J BUON 16(2): 274-276.

Ito M, Yoshida K, Kyo E, et al. 1990. Expression of several growth factors and their receptor genes in human colon carcinomas. Virchows Arch B Cell Pathol Incl Mol Pathol 59(3): 173-178.
https://doi.org/10.1007/BF02899402

Jiang L, Zhang J, Xu Q, et al. 2021. YAP promotes the proliferation and migration of colorectal cancer cells through the Glut3/AMPK signaling pathway. Oncol Lett 21(4): 312.
https://doi.org/10.3892/ol.2021.12573

Jozwiak P, Krzeslak A, Pomorski L, et al. 2012. Expression of hypoxia-related glucose transporters GLUT1 and GLUT3 in benign, malignant and non-neoplastic thyroid lesions. Mol Med Rep 6(3): 601-606.
https://doi.org/10.3892/mmr.2012.969

Kang I, Lee BC, Choi SW, et al. 2018. Donor-dependent variation of human umbilical cord blood mesenchymal stem cells in response to hypoxic preconditioning and amelioration of limb ischemia. Exp Mol Med 50(4): 1-15.
https://doi.org/10.1038/s12276-017-0014-9

Karageorgis G, Reckzeh ES, Ceballos J, et al. 2018. Chromopynones are pseudo natural product glucose uptake inhibitors targeting glucose transporters GLUT-1 and -3. Nat Chem 10(11): 1103-1111.
https://doi.org/10.1038/s41557-018-0132-6

Kawauchi K, Araki K, Tobiume K, et al. 2008. p53 regulates glucose metabolism through an IKK-NF-kappaB pathway and inhibits cell transformation. Nat Cell Biol 10(5): 611-618.
https://doi.org/10.1038/ncb1724

Unedited

Kayano T, Fukumoto H, Eddy RL, et al. 1988. Evidence for a family of human glucose transporter-like proteins. Sequence and gene localization of a protein expressed in fetal skeletal muscle and other tissues. J Biol Chem 263(30): 15245-15248.

Kim E, Jung S, Park WS, et al. 2019. Upregulation of SLC2A3 gene and prognosis in colorectal carcinoma: analysis of TCGA data. BMC Cancer 19(1): 302.
https://doi.org/10.1186/s12885-019-5475-x

Kuo CC, Ling HH, Chiang MC, et al. 2019. Metastatic Colorectal Cancer Rewrites Metabolic Program Through a Glut3-YAP-dependent Signaling Circuit. Theranostics 9(9): 2526-2540.
https://doi.org/10.7150/thno.32915

Li T, Guo T, Liu H, et al. 2021. Plateletderived growth factorBB mediates pancreatic cancer malignancy via regulation of the Hippo/Yesassociated protein signaling pathway. Oncol Rep 45(1): 83-94.
https://doi.org/10.3892/or.2020.7859

Liang YY, Deng XB, Lin XT, et al. 2020. RASSF1A inhibits PDGFB-driven malignant phenotypes of nasopharyngeal carcinoma cells in a YAP1-dependent manner. Cell Death Dis 11(10): 855.
https://doi.org/10.1038/s41419-020-03054-z

Liberti MV and Locasale JW 2016. The Warburg Effect: How Does it Benefit Cancer Cells? Trends Biochem Sci 41(3): 211-218.
https://doi.org/10.1016/j.tibs.2015.12.001

Liu JY, Li YH, Lin HX, et al. 2013. Overexpression of YAP 1 contributes to progressive features and poor prognosis of human urothelial carcinoma of the bladder. BMC Cancer 13: 349.
https://doi.org/10.1186/1471-2407-13-349

Livak KJ and Schmittgen TD 2001. Analysis of relative gene expression data using real-time quantitative PCR and the 2(-Delta Delta C(T)) Method. Methods 25(4): 402-408.
https://doi.org/10.1006/meth.2001.1262

Lu J 2019. The Warburg metabolism fuels tumor metastasis. Cancer Metastasis Rev 38(1-2): 157-164.
https://doi.org/10.1007/s10555-019-09794-5

Martinez-Romero J, Bueno-Fortes S, Martin-Merino M, et al. 2018. Survival marker genes of colorectal cancer derived from consistent transcriptomic profiling. BMC Genomics 19(Suppl 8): 857.
https://doi.org/10.1186/s12864-018-5193-9

McCarty MF, Somcio RJ, Stoeltzing O, et al. 2007. Overexpression of PDGF-BB decreases colorectal and pancreatic cancer growth by increasing tumor pericyte content. J Clin Invest 117(8): 2114-2122.
https://doi.org/10.1172/JCI31334

Nakamura Y, Tanaka F, Yoshikawa Y, et al. 2008. PDGF-BB is a novel prognostic factor in colorectal cancer. Ann Surg Oncol 15(8): 2129-2136.
https://doi.org/10.1245/s10434-008-9943-9

Neri S, Miyashita T, Hashimoto H, et al. 2017. Fibroblast-led cancer cell invasion is activated by epithelial-mesenchymal transition through platelet-derived growth factor BB secretion of lung adenocarcinoma. Cancer Lett 395: 20-30.
https://doi.org/10.1016/j.canlet.2017.02.026

Novakovic B, Gordon L, Robinson WP, et al. 2013. Glucose as a fetal nutrient: dynamic regulation of several glucose transporter genes by DNA methylation in the human placenta across gestation. J Nutr Biochem 24(1): 282-288.
https://doi.org/10.1016/j.jnutbio.2012.06.006

Pan J and Zang Y 2022. LINC00667 Promotes Progression of Esophageal Cancer Cells by Regulating miR-200b-3p/SLC2A3 Axis. Dig Dis Sci 67(7): 2936-2947.
https://doi.org/10.1007/s10620-021-07145-5

Parnaby CN, Bailey W, Balasingam A, et al. 2012. Pulmonary staging in colorectal cancer: a review. Colorectal Dis 14(6): 660-670.
https://doi.org/10.1111/j.1463-1318.2011.02601.x

Reckzeh ES, Karageorgis G, Schwalfenberg M, et al. 2019. Inhibition of Glucose Transporters and Glutaminase Synergistically Impairs Tumor Cell Growth. Cell Chem Biol 26(9): 1214-1228 e1225.
https://doi.org/10.1016/j.chembiol.2019.06.005

Segarra-Mondejar M, Casellas-Diaz S, Ramiro-Pareta M, et al. 2018. Synaptic activity-induced glycolysis facilitates membrane lipid provision and neurite outgrowth. EMBO J 37(9).
https://doi.org/10.15252/embj.201797368

Shan H, Takahashi T, Bando Y, et al. 2011. Inhibitory effect of soluble platelet-derived growth factor receptor beta on intraosseous growth of breast cancer cells in nude mice. Cancer Sci 102(10): 1904-1910.
https://doi.org/10.1111/j.1349-7006.2011.02026.x

Shi Y, Zhang Y, Ran F, et al. 2020. Let-7a-5p inhibits triple-negative breast tumor growth and metastasis through GLUT12-mediated warburg effect. Cancer Lett 495: 53-65.
https://doi.org/10.1016/j.canlet.2020.09.012

Siegel RL, Miller KD, Fuchs HE, et al. 2022. Cancer statistics, 2022. CA Cancer J Clin 72(1): 7-33.
https://doi.org/10.3322/caac.21708

Simpson IA, Dwyer D, Malide D, et al. 2008. The facilitative glucose transporter GLUT3: 20 years of distinction. Am J Physiol Endocrinol Metab 295(2): E242-253.

Unedited

https://doi.org/10.1152/ajpendo.90388.2008
Song N, Huang Y, Shi H, et al. 2009. Overexpression of platelet-derived growth factor-BB increases tumor pericyte content via stromal-derived factor-1alpha/CXCR4 axis. Cancer Res 69(15): 6057-6064.
https://doi.org/10.1158/0008-5472.CAN-08-2007
Stavri GT, Hong Y, Zachary IC, et al. 1995. Hypoxia and platelet-derived growth factor-BB synergistically upregulate the expression of vascular endothelial growth factor in vascular smooth muscle cells. FEBS Lett 358(3): 311-315.
https://doi.org/10.1016/0014-5793(94)01458-d
Sullivan CR, Koene RH, Hasselfeld K, et al. 2019. Neuron-specific deficits of bioenergetic processes in the dorsolateral prefrontal cortex in schizophrenia. Mol Psychiatry 24(9): 1319-1328.
https://doi.org/10.1038/s41380-018-0035-3
Sun Z, Ou C, Liu J, et al. 2019. YAP1-induced MALAT1 promotes epithelial-mesenchymal transition and angiogenesis by sponging miR-126-5p in colorectal cancer. Oncogene 38(14): 2627-2644.
https://doi.org/10.1038/s41388-018-0628-y
Tahir SA, Yang G, Goltsov A, et al. 2013. Caveolin-1-LRP6 signaling module stimulates aerobic glycolysis in prostate cancer. Cancer Res 73(6): 1900-1911.
https://doi.org/10.1158/0008-5472.CAN-12-3040
Triozzi PL, Stirling ER, Song Q, et al. 2022. Circulating Immune Bioenergetic, Metabolic, and Genetic Signatures Predict Melanoma Patients' Response to Anti-PD-1 Immune Checkpoint Blockade. Clin Cancer Res 28(6): 1192-1202.
https://doi.org/10.1158/1078-0432.CCR-21-3114
Wang H, Du YC, Zhou XJ, et al. 2014. The dual functions of YAP-1 to promote and inhibit cell growth in human malignancy. Cancer Metastasis Rev 33(1): 173-181.
https://doi.org/10.1007/s10555-013-9463-3
Wang KJ, Wang C, Dai LH, et al. 2019. Targeting an Autocrine Regulatory Loop in Cancer Stem-like Cells Impairs the Progression and Chemotherapy Resistance of Bladder Cancer. Clin Cancer Res 25(3): 1070-1086.
https://doi.org/10.1158/1078-0432.CCR-18-0586
Wang W, Xiao ZD, Li X, et al. 2015. AMPK modulates Hippo pathway activity to regulate energy homeostasis. Nat Cell Biol 17(4): 490-499.
https://doi.org/10.1038/ncb3113
Wellberg EA, Johnson S, Finlay-Schultz J, et al. 2016. The glucose transporter GLUT1 is required for ErbB2-induced mammary tumorigenesis. Breast Cancer Res 18(1): 131.
https://doi.org/10.1186/s13058-016-0795-0
Wu B, Tao L, Yang D, et al. 2020. Development of an Immune Infiltration-Related Eight-Gene Prognostic Signature in Colorectal Cancer Microenvironment. Biomed Res Int 2020: 2719739.
https://doi.org/10.1155/2020/2719739
Yang M, Guo Y, Liu X, et al. 2020. HMGA1 Promotes Hepatic Metastasis of Colorectal Cancer by Inducing Expression of Glucose Transporter 3 (GLUT3). Med Sci Monit 26: e924975.
https://doi.org/10.12659/MSM.924975
Yao PA, Wu Y, Zhao K, et al. 2022. The feedback loop of ANKHD1/lncRNA MALAT1/YAP1 strengthens the radioresistance of CRC by activating YAP1/AKT signaling. Cell Death Dis 13(2): 103.
https://doi.org/10.1038/s41419-022-04554-w
Ye Y, Zhang R and Feng H 2020. Fibronectin promotes tumor cells growth and drugs resistance through a CDC42-YAP-dependent signaling pathway in colorectal cancer. Cell Biol Int 44(9): 1840-1849.
https://doi.org/10.1002/cbin.11390
Yi B, Williams PJ, Niewolna M, et al. 2002. Tumor-derived platelet-derived growth factor-BB plays a critical role in osteosclerotic bone metastasis in an animal model of human breast cancer. Cancer Res 62(3): 917-923.
Yoo W, Lee J, Jun E, et al. 2019. The YAP1-NMU Axis Is Associated with Pancreatic Cancer Progression and Poor Outcome: Identification of a Novel Diagnostic Biomarker and Therapeutic Target. Cancers (Basel) 11(10).
https://doi.org/10.3390/cancers11101477
Younes M, Lechago LV, Somoano JR, et al. 1997. Immunohistochemical detection of Glut3 in human tumors and normal tissues. Anticancer Res 17(4A): 2747-2750.
Zhang Y, Cedervall J, Hamidi A, et al. 2020. Platelet-Specific PDGFB Ablation Impairs Tumor Vessel Integrity and Promotes Metastasis. Cancer Res 80(16): 3345-3358.
https://doi.org/10.1158/0008-5472.CAN-19-3533

Unedited